Luminescence investigation of Pr^{3+}-activated $InTaO_4$ red-emitting phosphor for white light emitting diodes

AN TANG[1,*], YONG TIAN[2], QILI FAN[3], XIDONG LIU[1]
[1]*Department of Mechanical Engineering, Henan University of Engineering, Zhengzhou, Henan 451191, China*
[2]*Department of Mechanical & Electrical Engineering, Henan Mechanical and Electrical Vocational College, Zhengzhou, Henan, 451191, China*
[3]*Department of Electrical and Electronic Engineering, Zhengzhou Technical College, Zhengzhou Henan 450121, China*

A series of Pr^{3+}-activated red-emitting phosphors $InTaO_4$:xPr^{3+} were prepared by a conventional solid-state reaction technique. The structure, the particle size distribution, and photoluminescence properties of these samples have been respectively researched by X-ray diffraction (XRD), laser size distribution analyzer and molecular fluorescence spectrometer. The as-gotten phosphor has a monoclinic crystal structure with single phase and its mean particle size is approximately 2.2μm, which is suitable for manufacture of the solid-lighting devices. The phosphor can be effectively excited by the blue lights of 451nm and 465nm, and emit red strong red lights at 603nm and 614nm. The emission intensities of the phosphors $InTaO_4$:xPr^{3+} increase with enhancing doping Pr^{3+} content and get a maximum value when x is 0.006, then decrease with the addition of Pr^{3+}. The CIE chromaticity coordinates (0.65, 0.32) of the phosphor $InTaO_4$:0.004Pr^{3+} are near to the ideal coordinates (0.67, 0.33). The phosphor $InTaO_4$:0.004Pr^{3+} is probably considered to be a potential red-emitting conversion phosphor for white light emitting diodes (LEDs).

(Received January 15, 2023; accepted February 12, 2024)

Keywords: Pr^{3+}-activated red-emitting phosphor, Photoluminescence properties, $InTaO_4$; Solid-state reaction, White LEDs

1. Introduction

Compared with traditional lighting technology, white light emitting diodes (LEDs) have many advantages, such as energy saving, easy production, long life, and no environmental pollution. So white LEDs are regarded as a new generation of lighting source that meets the requirements of green lighting [1-4]. Presently white LEDs can be obtained by the following four methods [5-9]: phosphor conversion method, "red, green, blue (RGB)" multi chip method, quantum-well method and white organic LEDs (OLEDs) method. The latter three methods are limited in their application due to their several difficulties, including low light efficiency and high cost [10]. For this reason, the fluorescent conversion method to produce white LEDs is relatively simple in operation, low in cost, and easy to realize industrial production, and it is favored by people and has become one of the research focuses.

There are two main ways to obtain white LEDs through the phosphor conversion method [11, 12]: one is a blue LED plus yellow phosphor, the other is a near-ultraviolet (n-UV) LED with red, green and blue phosphors. In these methods, the red phosphor plays a key role in adjusting the color temperature of white LEDs and improving the color rendering property. Currently, the commercial red phosphors for white LEDs are mainly Y_2O_2S:Eu^{3+} [13-15]. In contrast to the blue phosphors ZnS:(Cu^+, Al^{3+}) and the green phosphors $BaMgAl_{10}O_{17}$:Eu^{2+} (BAM), the red phosphors Y_2O_2S:Eu^{3+} mainly have the following disadvantages [16-20]: low luminous efficiency, pour absorption effect of near ultraviolet excitation, and unstable chemical property with the sulfide gas releasing when the excitation light is irradiated, which affects the service life of LED. Therefore, it is very important to develop a new red phosphor with a better luminescence performance for white LEDs.

Exploring a new type of red phosphor for white LEDs doped with Pr^{3+} has aroused the interest of researchers. The electronic layer structure of Pr^{3+} is $[Xe]4f^2$ [21]. Pr^{3+} ions have rich energy level transitions, and their luminescence spectra have the characteristics of multiple spectral lines. For example [22-24], the transitions of $^1S_0 \rightarrow {}^3H_4$, $^3P_0 \rightarrow {}^3H_4$, $^1D_2 \rightarrow {}^3H_4$ respectively generate blue light, green light and red light. The luminous color and intensity of Pr^{3+} are closely related to the crystal structure of the substrate. In this paper, luminescence properties of Pr^{3+}-activated $InTaO_4$ red phosphor for white LEDs were reported.

2. Experimental

2.1. Preparation of $InTaO_4:xPr^{3+}$ phosphors

Samples of $InTaO_4:xPr^{3+}$ phosphors were prepared by a conventional high temperature solid-state reaction approach. The starting stoichiometric materials were indium oxide (In_2O_3, 99.99%, purchased from Meryer (Shanghai) Biochemical Technology Co., Ltd.), tantalum oxide (Ta_2O_5, analytical grade, purchased from Sinopharm Chemical Reagent Co., Ltd.), and praseodymium oxide (Pr_6O_{11}, 99.99%, purchased from China General Research Institute for Nonferrous Metals). These materials were weighed and poured into an agate mortar to mix. Each sample was triturated for about 20min, then the homogeneous mixture was put into an alumina crucible. The mixtures were firstly preheated for 4h at 600℃ and next calcined for 6h at 1200℃ in a resistance furnace. Finally the $InTaO_4:xPr^{3+}$ phosphor samples were obtained after they were cooled in the air with the furnace.

2.2. Characterization of $InTaO_4:xPr^{3+}$ phosphors

Powder X-ray diffraction (XRD) was used to examine the structure of the final sample on a Shimadzu XRD-6000 diffractometer with Cu Kα radiation at 40kV and 150mA. The particle size distribution was characterized by Shimadzu SA-CP3 laser size distribution analyzer. The excitation and emission spectra were measured on an RF-5301 molecular fluorescence spectrometer using a Xe lamp as the excitation source with the slit width of 3nm. All the measurements were done at room temperature in air.

3. Results and discussion

3.1. XRD and size distribution analysis

Fig. 1 shows the XRD pattern of $InTaO_4:0.004Pr^{3+}$ phosphor. All diffracted peaks are similar to the Joint Committee on Powder Diffraction Standards (JCPDS) (No. 81-1196). According to the JCPDS, $InTaO_4$ has a monoclinic crystal structure and a space group of *P2/a (13)*. The sample is single $InTaO_4$ phase and second phase is hardly observed. Due to the same valence states between In^{3+} and Pr^{3+}, and in consideration of the ion sizes of In^{3+} (0.080nm), Pr^{3+} (0.113nm) and Ta^{5+} (0.064nm), the doped Pr^{3+} ions occupied the In^{3+} sites in this phosphor. The result of the XRD also illustrates that a little amount of added Pr^{3+} has almost no influence on the host structure $InTaO_4$ and the major diffraction of peaks have no shift to the side of the lower or higher angles, which may be attributed to the similar ionic radius of Pr^{3+} as compared to that of In^{3+} and the extra small amount of doped Pr^{3+} ions. In this experimental, the $InTaO_4:xPr^{3+}$ phosphor was synthesized successfully.

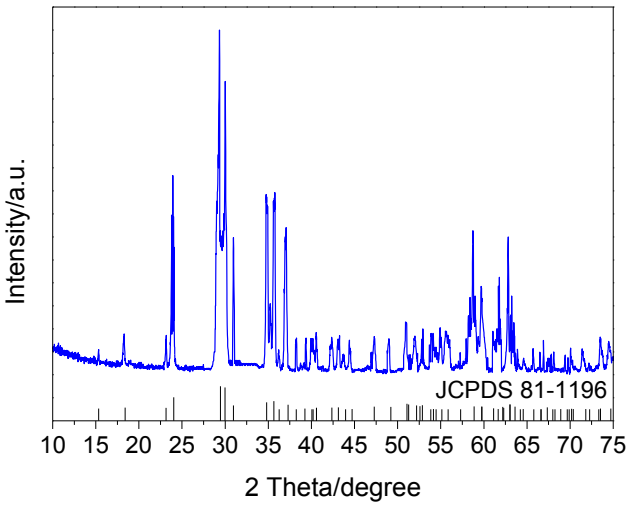

Fig. 1. X-ray diffraction pattern of the phosphor $InTaO_4:0.004Pr^{3+}$ (color online)

Fig. 2 gives the particle size distribution of the phosphor $InTaO_4:0.004Pr^{3+}$. The distribution has a narrow size with an average diameter of approximate 2.2μm, which is fit to coat the solid-lighting devices [25].

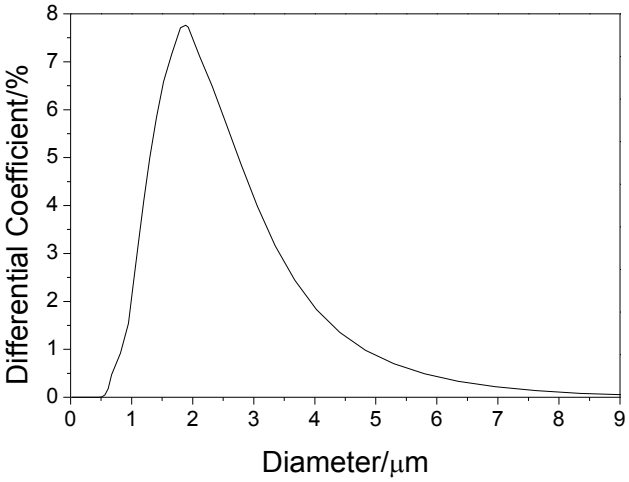

Fig. 2. Particle size distribution of the phosphor $InTaO_4:0.004Pr^{3+}$

3.2. Photoluminescence properties

Fig. 3 shows the spectrum of the phosphor $InTaO_4:0.004Pr^{3+}$ under the monitoring of 615nm light. It can be seen that there are three obvious sharp peaks in the figure, which represent the typical f-f transition of Pr^{3+} that is composed of $^3H_4 \rightarrow {}^3P_J$ (J=0, 1, 2). These intense peaks are located at about 451nm ($^3H_4 \rightarrow {}^3P_2$), 479nm ($^3H_4 \rightarrow {}^3P_1$) and 491nm ($^3H_4 \rightarrow {}^3P_0$). Among these energy level transitions, $^3H_4 \rightarrow {}^3P_2$ is hypersensitive transitions, which is sensitive to the surrounding environment. If Pr^{3+} ions perch on the symmetrical center, such sharp peaks do not exist. At the same time, several

sharps of the low intensity are also observed. This phenomenon is named as sub level state caused by the splitting of some energy levels in the excited state. The above wavelengths well match the wavelength of blue LED chip emission, which is indicative of the phosphor $InTaO_4:xPr^{3+}$ effectively excited by commercial LED chip.

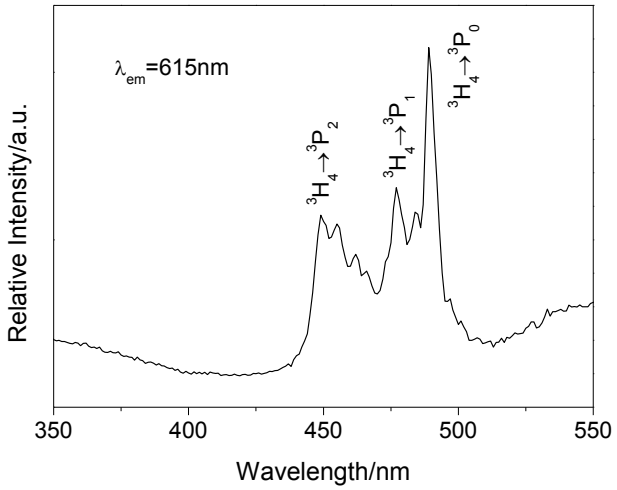

Fig. 3. Excitation spectrum of the phosphor $InTaO_4:0.004Pr^{3+}$

Fig. 4 represents the emission spectrum of the phosphor $InTaO_4:0.004Pr^{3+}$ under the excitation wavelength at 451nm. There are two strong peaks seen in the emission spectrum, which are separately around 603nm ($^1D_2 \rightarrow {}^3H_4$) and 614nm ($^3P_0 \rightarrow {}^3H_6$). The light of these two wavelengths is the range of red light, indicating that the obtained phosphor $InTaO_4:xPr^{3+}$ can emit high intensity red light with the irradiation of blue light. In other words, the phosphor $InTaO_4:xPr^{3+}$ is possible to be used in the production field of white LEDs.

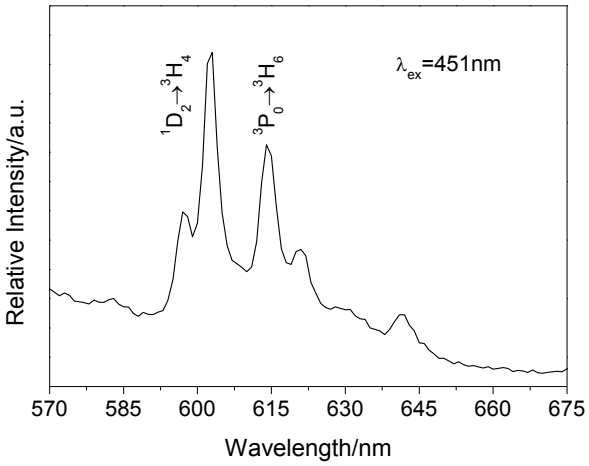

Fig. 4. Emission spectrum of the phosphor $InTaO_4:0.004Pr^{3+}$

3.3. Effect of Pr^{3+} content on the photoluminescence properties

Fig. 5 brings the effect of different Pr^{3+} content in the phosphors $InTaO_4:xPr^{3+}$ (x=0.001, 0.002, 0.003, 0.004, 0.005, 0.006) on the photoluminescence intensity at the highest $^1D_2 \rightarrow {}^3H_4$ transition of the Pr^{3+} with the wavelength at 603nm.

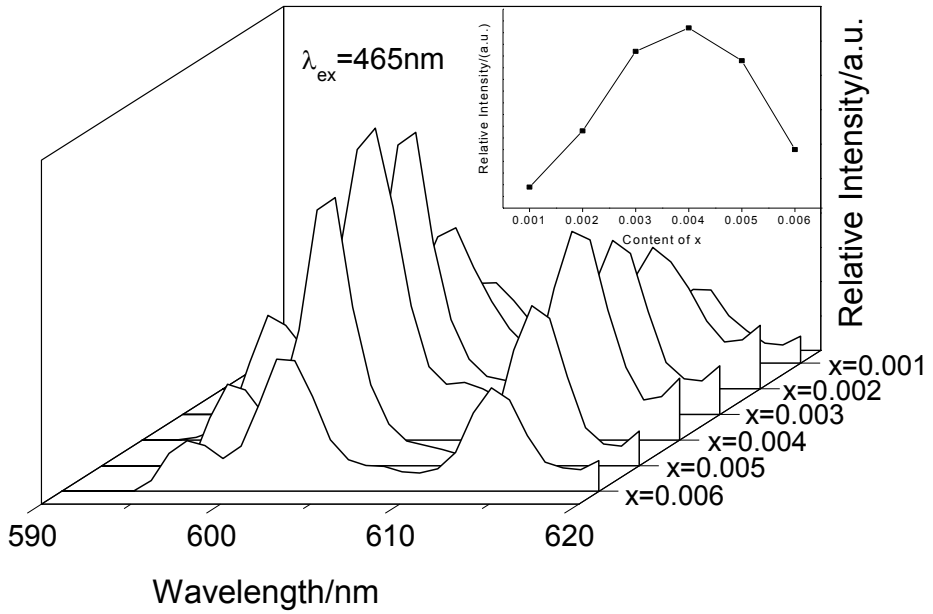

Fig. 5. Effect of Pr^{3+} content on photoluminescence of the phosphors $InTaO_4:xPr^{3+}$ (x=0.001, 0.002, 0.003, 0.004, 0.005, 0.006). The inset shows the emission intensities of the phosphors with different Pr^{3+} doping contents

From the picture, the emission shapes and peak positions do not change as the Pr^{3+} content varies except for the emission intensity. A low doping Pr^{3+} content gives weak luminescence intensity, and the photoluminescence intensity enhances along with the increase of the Pr^{3+} content. The intensity reaches a maximum when the x value is 0.004. Once x is in excess of 0.004, the photoluminescence intensity diminishes contrarily. An over Pr^{3+} doping content creates the luminescence quenching attributing to energy migration among Pr^{3+} ions because of the enhancement of non-radiative relaxation between the neighboring Pr^{3+} ions under the doping concentration increase [26, 27]. Seen from this angle, the optimum content of Pr^{3+} in the phosphors $InTaO_4$:xPr^{3+} is x=0.004 in this work.

Fig. 6 demonstrates the CIE chromaticity coordinates of the phosphor $InTaO_4$:0.004Pr^{3+} calculated according to the CIE standards and the coordinates are x=0.65, y=0.32, which approximates to the ideal coordinates (0.67, 0.33) of the red light. For this reason, the synthesized red phosphor is binding on the application for white LEDs.

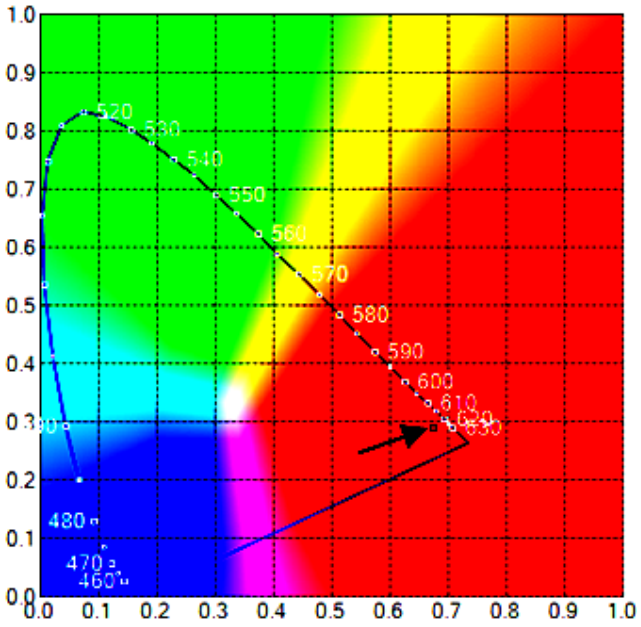

Fig. 6. CIE chromaticity coordinates of the phosphor $InTaO_4$:0.004Pr^{3+} (color online)

4. Conclusions

In conclusion, Pr^{3+}-doped $InTaO_4$:xPr^{3+} (x=0.001, 0.002, 0.003, 0.004, 0.005, 0.006) phosphors were successfully synthesized by a traditional solid-state reaction technique in high temperature air. X-ray measurement illustrates that the phosphors are of single phase. The excitation spectrum shows that the phosphor can be excited efficiently by the blue lights of 451nm and 465nm. The emission spectrum demonstrates that the phosphor can emit intensive red lights at 603nm and 614nm by the excitation of the blue light. With the addition of the Pr^{3+}, the emission intensities of the phosphors $InTaO_4$:xPr^{3+} strongly increase and reach the maximum at x=0.004. The CIE chromaticity coordinates (0.65, 0.32) are more close to the ideal coordinates (0.67, 0.33). All the results show that the phosphor $InTaO_4$:0.004Pr^{3+} is more suitable for applications in the area of white LEDs.

Acknowledgements

This work was supported by Key Scientific Research Projects of Colleges and Universities in Henan Province (22A430016).

References

[1] L. Li, Q. W. Cao, J. J. Wang, Z. Y. Li, Y. Pan, X. T. Wei, Y. Wei, Ceram. Int. **48**, 36140(2022).
[2] Z. Han, X. Y. Wang, B. Fu, H. K. Yan, J. S. Liao, J. Lumin. **252**, 119405(2022).
[3] J. H. Xie, J. Q. Cheng, H. Tang, X. F. Yu, Z. X. Wang, X. Y. Mi, Q. S. Liu, X. Y. Zhang, J. Alloy Compd. **882**, 160589 (2021).
[4] Z. G. Xia, R. S. Liu, J. Phys. Chem. C **116**, 15604 (2012).
[5] Y. Bi, S. Y. Chen, H. Zhao, X. Y. Zhang, J. Mater. Sci. **33**, 23075(2022).
[6] A. K. Bedyal, V. Kumar, H. C. Swart, Physica B **535**, 189(2018).
[7] H. C. Kuo, C. W. Hung, H. C. Chen, K. J. Chen, C. H. Wang, C. W. Sher, C. C. Yeh, C. C. Lin, C. H. Chen, Y. J. Cheng, Opt. Express. **19**, A930 (2011).
[8] Y. J. Hua, X. J. Li, D. W. Zhang, H. P. Ma, D. G. Deng, S. Q. Xu, New J. Chem. **40**, 5458 (2016).
[9] N. Deopa, S. Kaur, A. Prasad, B. Joshi, A. S. Rao, Opt. Laser Technol. **108,** 434(2018).
[10] P. Suthanthirakumar, K. Marimuthu, J. Mol. Struct. **1125**, 443(2016).
[11] S. Y. Zhang, P. Y. Zhang, Y. L. Huang, H. J. Seo, J. Lumin. **207**, 460(2019).
[12] M. Yan, D. C. Zhu, Y. Pu, Q. Yan, Optik **229**, 166250 (2021).
[13] W. Z. Sun, R. Pang, H. F. Li, Y. L. Jia, S. Zhang, L. H. Jiang, C. Y. Li, J. Rare Earth. **33**, 814 (2015).
[14] Z. Y. Cao, S. J. Dong, S. K. Shi, J. Y. Wang, L. S. Fu, J. Solid State Chem. **307**, 122840 (2022).
[15] W. Xie, J. H. Li, H. Y. Ni, Q. H. Zhang, Opt. Mater. **118**, 111240 (2021).
[16] B. Fan, W. X. Zhou, S. M. Qi, J. Solid State Chem. **283**, 121158 (2020).

[17] T Wang, X. H. Xu, D. C. Zhou, J. B. Qiu, X. Yu, Mater. Res. Bull. **60**, 876 (2014).
[18] P. Du, J. S. Yu, Dyes Pigments. **147**, 16 (2017).
[19] C. Ding, W. J. Tang, Opt. Mater. **76**, 56 (2018).
[20] W. Y. Yuan, J. J. Fan, L. J. Dong, S. H. Chen, X. J. Fan, G. Q. Zhang, Microelectron Reliab. **121**, 114130 (2021).
[21] F. B. Xiong, S. D. Chen, W. B. Yang, X. G. Meng, Opt. Mater. **128**, 112390(2022).
[22] S. Y. Liu, M. H. Wu, W. Chen, Y. C. Sun, Z. S. Zheng, G. L. Chen, Y. H. Zeng, L. F. Huang, J. Solid State Chem. **294**, 121861(2021).
[23] R. Gopal, J. Manam, Ceram. Int. **48**, 30724 (2022).
[24] S. H. Xin, F. G. Zhou, C. Wang, X. J. Wang, Z. W. Li, G. Zhu, Y. H. Wang, J. Mol. Struct. **1181**, 203 (2019).
[25] R. P. Rao, Solid State Commun. **99**, 439 (1996).
[26] N. Mohamed, J. Hassan, K. A. Matori, R. S. Azis, Z. A. Wahab, Z. M. Mohd Ismail, N. F. Baharuddin, S. S. Abdul Rashid, Results Phys. **7**, 1202 (2017).
[27] Y. D. Xu, X. D. Peng, L. Wang, M. Shi, Y. Zhang, Q. Wang, S. Qi, N. Ding, Chin. J. Chem. **28**, 771 (2015).

*Corresponding author: tangan527@126.com